

See discussions, stats, and author profiles for this publication at: <https://www.researchgate.net/publication/238123574>

Rotational Dynamics of Linear Polysaccharides in Solution. ^{13}C Relaxation Study on Amylose and Inulin

ARTICLE in MACROMOLECULES · NOVEMBER 1995

Impact Factor: 5.8 · DOI: 10.1021/ma00127a055

CITATIONS

10

READS

14

4 AUTHORS, INCLUDING:



Photis Dais

University of Crete

124 PUBLICATIONS 2,102 CITATIONS

SEE PROFILE



Isabelle André

Institut National des Sciences Appliquées de ...

75 PUBLICATIONS 909 CITATIONS

SEE PROFILE

Rotational Dynamics of Linear Polysaccharides in Solution. ^{13}C Relaxation Study on Amylose and Inulin

Emmanuel Tylianakis and Photis Dais*

Department of Chemistry, University of Crete,
714 09 Iraklion, Crete, Greece

Isabell Andre and Francois F. Taravel*

Centre de Recherches sur les Macromolécules Végétales
(CERMAV), CNRS, BP 53, 38041 Grenoble Cedex 9, France

Received April 4, 1995

Revised Manuscript Received September 5, 1995

Introduction. This communication presents multi-field, variable-temperature ^{13}C NMR relaxation data of amylose in dimethyl sulfoxide and inulin in water solutions in an attempt to describe quantitatively their dynamics by employing various theoretical time correlation functions (TCF) or dynamic models. The second goal of this report is the discrimination of the various models used to describe the dynamics of amylose by extending the relaxation data set with respect to earlier relaxation measurements¹⁻³ carried out at one temperature. On the basis of the present relaxation data, a critical evaluation of the various dynamic models has been made regarding their ability to describe the chain segmental motions and internal rotation of the exocyclic hydroxymethyl groups of the two polysaccharides.

Experimental Section. Samples of potato amylose from Aldrich ($M_w = 3.3 \times 10^5$, $[\eta] = 104.7 \text{ mL/g}$), 10% (w/v) in $(\text{CH}_3)_2\text{SO}-d_6$, and inulin from Sigma ($M_w = 5.1 \times 10^3$, $[\eta] = 17 \text{ mL/g}$), 4% (w/v) in D_2O , were used in the present study.

^{13}C relaxation and NOE measurements were conducted with Bruker AC200, AC300, and AM400 spectrometers operating at 50.3, 75.4, and 100.5 MHz, respectively, for carbon-13 under broad-band proton decoupling. Experimental details for measuring ^{13}C T_1 , T_2 , and NOE are reported elsewhere.^{1,2} The sample temperature was controlled to within $\pm 1^\circ\text{C}$ by means of precalibrated thermocouples in the probe inserts.

All numerical calculations and fits to experimental data of amylose and inulin were achieved by using the Moldyn program⁴ modified to include the aforementioned models. Details for the optimization procedure and other aspects of the program as well as details of fitting procedures to the experimental relaxation data have been described in refs 1-3.

Results and Discussion. All the unimodal TCF's [$\log(\chi^2)$,⁵ diamond-lattice models,^{6,7} and conformational models⁸], as well as those reported in ref 2, which take explicitly into consideration the helix-like nature of the amylose in solution, failed to account for the experimental relaxation parameters, NT_1 , NT_2 (N being the number of protons attached to the carbon atom under consideration), and NOE, at the minimum in the curves of NT_1 as a function of temperature for the backbone carbons of amylose and inulin. However, the bimodal TCF developed by Dejean de la Batie, Laupretre, and Monnerie⁹ (DLM) proved to be a reasonable basis for the interpretation of the relaxation data of the backbone carbons of amylose and inulin at various temperatures and magnetic fields. The best fit NT_1 , NT_2 , and NOE data for the C-1 carbon of amylose and the C-3 carbon of inulin (Figure 1) are shown graphically in Figures 2

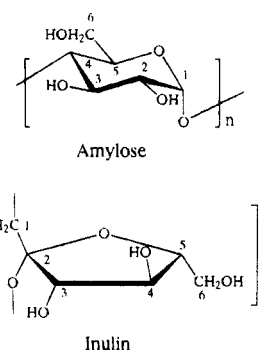


Figure 1. Structures of the principal repeat units of amylose and inulin.

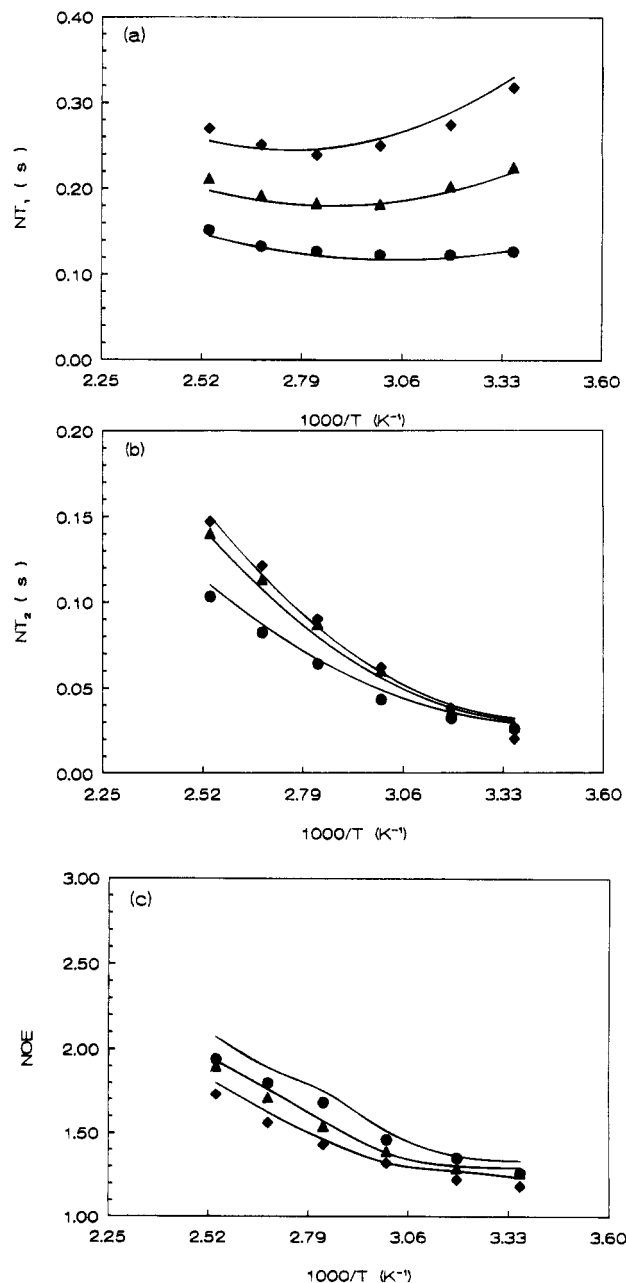


Figure 2. Temperature dependence of the experimental and calculated relaxation data of the C-1 carbon of amylose at (●) 50, (▲) 75, and (◆) 100 MHz: (a) NT_1 , (b) NT_2 , and (c) NOE data. Solid curves correspond to the DLM model fitting.

and 3, respectively. It is seen from these plots that good agreement between experimental and calculated values

* Authors to whom correspondence should be addressed.

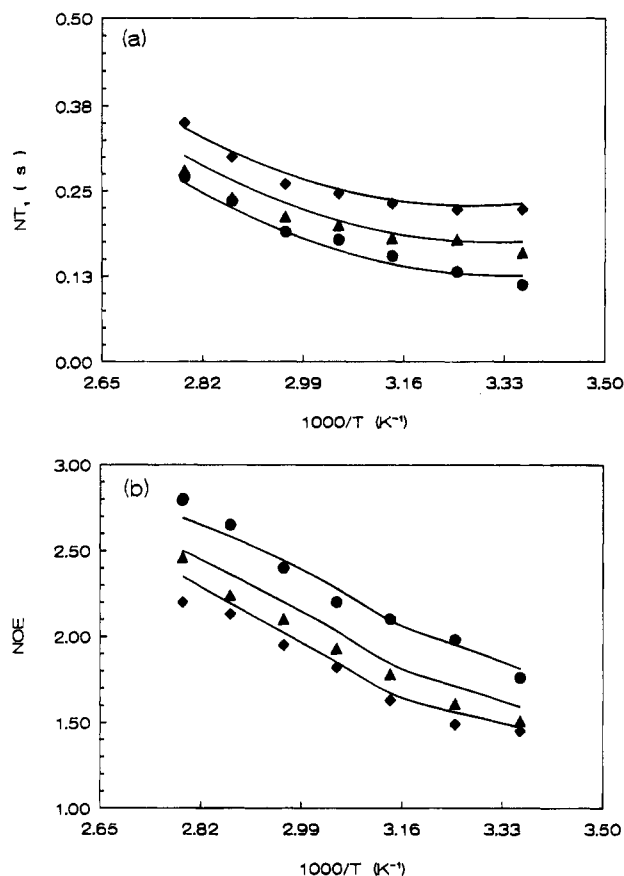


Figure 3. Temperature dependence of the experimental and calculated relaxation data of the C-3 carbon of amylose at (●) 50, (▲) 75, and (◆) 100 MHz: (a) NT_1 and (b) NOE data. Solid curves correspond to the DLM model fitting.

is obtained from this model throughout the entire temperature range studied. In all cases, the percent difference between the experimental and calculated values was within the experimental error ($\pm 10\%$) of the relaxation measurements. Similar good fittings were obtained for the remaining ring carbons of the two biopolymers (not shown).

The DLM model⁹ is an effective modification of the conformational jump model developed by Hall, Webber, and Helfand⁸ (HWH) by taking into consideration local anisotropic motion described by a fast libration of the C-H vectors in addition to segmental motion. The composite TCF of the DLM model and its Fourier transform, the spectral density, are given in the original paper.⁹ In this model, the time scale of chain segmental motion is set by two parameters, τ_0 and τ_1 , the correlation times in the HWH model describing single and cooperative transitions, respectively. The librational motion of the C-H vector has been described⁹ in terms of a fast, anisotropic motion occurring with correlation time τ_2 inside a cone of half-angle Θ , the axis of which coincides with the rest position of the C-H vector. For this model, the values of the fitting parameters are shown in Table 1. The simulated values for the angle Θ are 21.5° for the anomeric C-1 carbon and 27° , on the average, for the remaining ring carbons of amylose. The different values of Θ explain the fact that the NT_1 (and NT_2) values of the C-1 ring carbon are different from those of the other ring carbons, the latter being similar within experimental error. This observation supports earlier conclusions³ that these two carbon sites do not experience the same local dynamics. The smaller Θ value for the anomeric carbon indicates a greater steric

Table 1. Simulation Parameters of the DLM and Restricted Diffusion Models Used To Describe the Backbone Segmental Motion and Internal Rotation of Amylose and Inulin in Solutions

t ($^\circ\text{C}$)	amylose			inulin		
	τ_1 (10^{-10} s)	τ_1 (10^{-10} s)	χ^2	τ_1 (10^{-10} s)	τ_1 (10^{-10} s)	χ^2
25	45.73	0.67	37	17.54	0.42	62
35				13.82	0.34	71
40	39.28	0.54	39			
45				10.85	0.28	81
55				7.92	0.25	93
60	24.38	0.45	46			
65				5.91	0.21	107
75				4.47	0.20	102
80	14.13	0.32	52			
85				3.41	0.13	135
100	9.28	0.20	55			
120	5.85	0.18	57			
τ_0/τ_1	7			2		
τ_1/τ_2	100			90		
E_a (kJ mol $^{-1}$)	22	14		25	16	
corr coeff	0.99	0.97		0.99	0.98	

hindrance to the librational motion of the corresponding equatorial C-H vector relative to that of the axial vectors in the remaining ring sites. Shortening the C-1-O-1 and C-1-O-5 bonds relative to the remaining C-O bonds observed in the crystal structure of amylose¹⁰ and other α -glucopyranosides¹¹ appears to be a major cause for restricting the amplitude of the local libration at the anomeric carbon.

The C-3, C-4, and C-5 ring carbons of inulin are characterized by different NT_1 values. These differences, which are well outside the experimental error, indicate different local dynamics at the three ring carbon sites as expected from the pseudorotational concept linked to furanose rings.¹² This is reflected in the calculated Θ values for the librational motion of the corresponding C-H vectors, which are 26° , 29° , and 33° for the C-3-H-3, C-4-H-4, and C-5-H-5 vectors, respectively. The trend in the Θ values, which reflects the different magnitude of the steric hindrance to the librational motion on going from the C-3 to C-5 carbon sites, may be attributed to the relative position of the three C-H vectors with respect to the backbone chain of inulin. Experimental¹³⁻¹⁵ and theoretical^{13,16} studies on inulin have shown that the C-4-H-4 and C-5-H-5 vectors are progressively more remote from the main chain of inulin than the C-3-H-3 vector, and hence they experience a lesser steric hindrance from nonbonded interactions to their librational motion. Another explanation of the observed differentials in the librational angles of the various ring C-H vectors of inulin could be the presence of an intramolecular hydrogen-bonding arrangement within the fructofuranosyl ring of inulin. It has been found in the solid state¹⁵ that a plausible arrangement could involve intramolecular hydrogen bonding of OH-3 with the glycosidic linkage oxygen O-1 (strong), OH-3 with OH-4 (weak), and OH-6 with the ring oxygen O-5 (strong). However in solution, because of intermolecular association (solute-solvent) and ring flexibility, such intramolecular interactions are likely modified. In particular, the possible rotamer distribution (gauche-gauche, gauche-trans, and trans-gauche) around the C-5-C-6 bond could prevent the existence of the hydrogen bonding between the OH-6 hydroxyl and the O-5 oxygen. Nevertheless, the possible occurrence of intramolecular interactions of different intensity could explain the variation observed in the half-angles

for the librational motions of the C-3-H-3 and C-4-H-4 vectors relative to the C-5-H-5 vector.

The τ_1 values derived from fitting the experimental relaxation data for the ring carbons of amylose and inulin (Figures 2 and 3) with the DLM model are compiled in Table 1. These values when adjusted for the difference in solvent viscosity, indicate that the segmental motion of inulin is by a factor 2–3 faster than that of amylose at all temperatures, except perhaps at 25 °C. From Figure 1, which shows the structures of amylose and inulin, one may conclude that the –C–O–CH₂–C linkages connecting the inulin rings offer somewhat greater motional freedom than the simple C–O–C connecting the amylose rings. Plots of the logarithms of these values as a function of $1/T$ (K) show linear correlations, in the temperature range studied, yielding apparent activation energies, E_a , of 22 kJ mol^{–1} for amylose in dimethyl sulfoxide and 25 kJ mol^{–1} for inulin in water solutions. The activation energy, E^* , of the conformational transitions associated with the τ_1 correlation time can be estimated from the equation $E^* = E_a - \Delta H_\eta$, assuming that Kramers theory¹⁷ at the high-friction limit is valid for these polysaccharides. ΔH_η is the activation energy for the viscous flow and is 13 kJ mol^{–1} for dimethyl sulfoxide and 15 kJ mol^{–1} for water. This leads to values of barrier heights E^* of 9 and 10 kJ mol^{–1} for amylose and inulin, respectively. These values are similar to those for typical vinyl polymers, for which activation energies for segmental motion of about one barrier height have been observed. Activation energies of about one barrier crossing are commensurate with a type 2* transition according to Helfand's terminology.¹⁸

The ratio τ_0/τ_1 appears to decrease from amylose to inulin (Table 1), indicating that single conformational transitions associated with damping play a greater role on going from amylose to inulin biopolymer. Another interesting observation is the fact that the τ_1/τ_2 ratio decreases from amylose to inulin (Table 1), reflecting a decrease in the rate of the librational motion of the backbone C–H vectors from amylose to inulin. This result is in agreement with the observed best fit half-angles, Θ , of the librational motion, which increases on the average from 24° for amylose to 29° for inulin. A smaller half-angle corresponds to a shorter correlation time for the librational motion.¹⁹

Figure 4 shows plots of $\log(NT_1/\omega_C)$ vs $\log[\omega_C\tau_1(T)]$, reflecting the frequency–temperature superposition of the NT_1 data of amylose and inulin collected at different Larmor frequencies as suggested recently by Guillermo et al.²⁰ and others.^{19,21} Data from three Larmor frequencies superpose very well over the entire temperature range. The success of such a superposition demonstrates that all motional time constants contributing to spin relaxation are proportional to $\tau_1(T)$ and justifies attempts to fit the data to the TCF of the DLM model, the shape of which is independent of temperature.

It should be noted that the DLM model was not successful in reproducing the relaxation data of the backbone methylene C-1 carbon of inulin, unless the conic half-angle Θ was allowed to be an adjustable parameter at each temperature. However, as suggested by Dejean de la Batie et al.⁹ and verified through Brownian dynamics simulation by Adolf et al.,²² this librational motion, occurring on the time scale of picoseconds, arises from motion within dihedral potential wells, and hence it must be only very weakly dependent on the environment. Furthermore, this

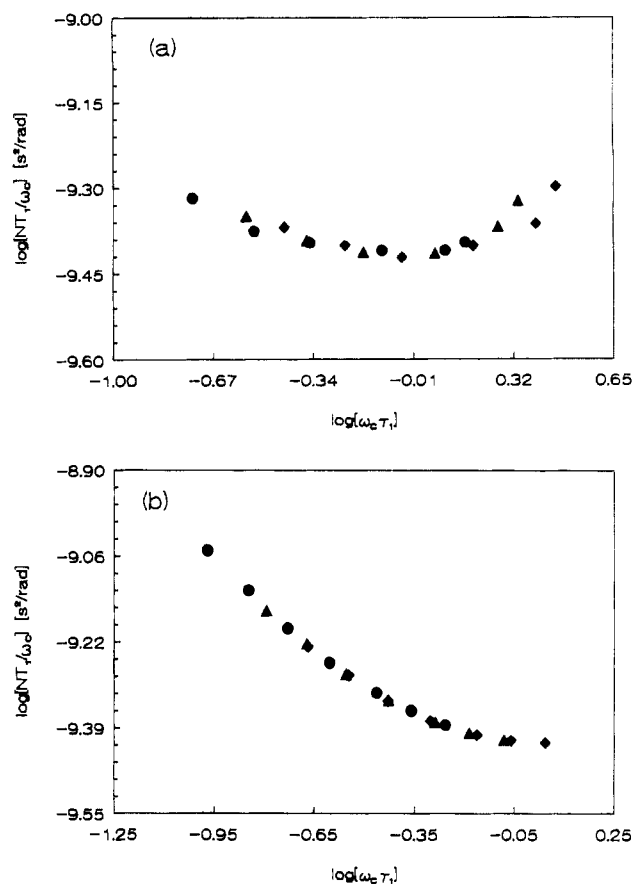


Figure 4. Frequency–temperature superposition of the backbone NT_1 data for (a) amylose and (b) inulin.

motion is too rapid to reflect thermally activated processes.²¹ Therefore, Θ is expected to be independent of the temperature. This assumption is supported experimentally by the relaxation time ratios, $T_1(\text{C-}i)/T_1(\text{C-}1)$ ($i = 3-5$), of the C-1 carbon (moderated by two protons) and the C-3, C-4, and C-5 ring carbons, which are less than the theoretical value of 2, and they remain essentially constant over the whole temperature range studied. For instance, the relaxation time ratios at 200 MHz, corresponding to the C-3, C-4, and C-5 ring carbons, were found to be 1.52 ± 0.09 , 1.65 ± 0.07 , and 1.82 ± 0.09 , respectively. Apparently, internal rotations about the C–O–C–1–C bonds of the linkage contribute to the relaxation of the backbone methylene C-1 carbon.

The internal motion of the hydroxymethyl groups of amylose and inulin about the exocyclic C-5–C-6 bonds superimposed on segmental motion could not be described by assuming free rotation of 360° about this bond. Composite TCF's²³ based on the HWH model and the Woessner equations²⁴ for stochastic diffusion and jump processes did not reproduce the experimental data for the C-6 carbon of amylose and inulin. This internal motion is expected to be of restricted amplitude owing to possible intramolecular and/or intermolecular hydrogen bonding, unfavorable nonbonded, and electrostatic interactions. For this reason, two other TCF's describing internal motion of restricted amplitude were used in the present analysis. The first model, the internal two-state jump model, developed by London,²⁵ describes internal jumps between two stable states, A and B, with lifetimes τ_A and τ_B . This motion of amplitude 2χ (i.e., jumps in between $-\chi$ and $+\chi$), assumed to be independent, is superimposed on segmental motion that may

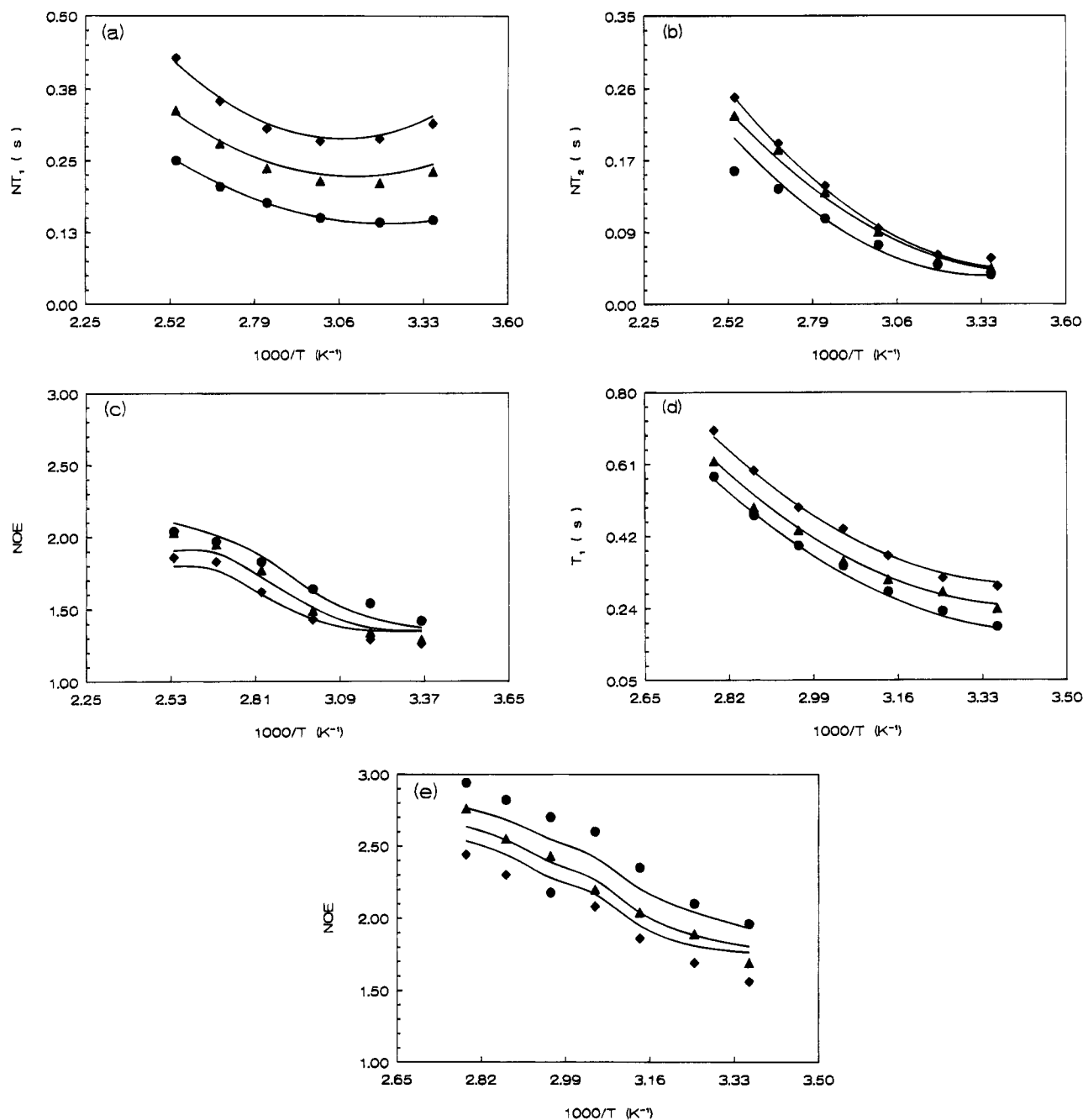


Figure 5. Temperature dependence of the experimental and calculated relaxation data of the exocyclic C-6 carbons of amylose and inulin at (●) 50, (▲) 75, and (◆) 100 MHz: (a) NT_1 , (b) NT_2 , and (c) NOE data for amylose; (d) NT_1 and (e) NOE data for inulin. Solid curves correspond to the restricted diffusion model fitting.

be described by the HWH model. The composite TCF of this model is given explicitly in ref 3. The second model for the movement of the hydroxymethyl group is "restricted-amplitude internal diffusion", i.e., continuous movement of O-6 between two limiting values of χ (2χ is the amplitude of the restricted diffusion about the C-5–C-6 bond). Restricted diffusion about a single axis has been solved analytically,^{26,27} and the resulting TCF can be combined with the TCF of the HWH model to give a new composite TCF,³ which incorporates the correlation time, τ_i , associated with internal motion and the allowed range of motion, 2χ .

Both models were able to reproduce the NT_1 and NOE experimental data of the C-6 carbons of amylose and inulin. However, only the diffusion model was successful in reproducing the experimental NT_2 data of the hydroxymethyl carbon of amylose. Also, the restricted

diffusion model is favored for two additional reasons. First, it requires fewer adjustable parameters than the two-state jump model in order to fit the data, and second, the fitting by the latter model resulted in physically unrealistic values of the correlation times, which did not follow an Arrhenius-type behavior. It should be noted that the restricted diffusion model fulfilled the important criterion²⁶ for its application to the present analysis; i.e., no discrepancy was found between the calculated relaxation parameters, NT_1 , NT_2 , and NOE, corresponding to a full range of motion ($2\chi = 360^\circ$), and the parameters derived by using the free internal rotation model.

Figure 5 shows plots of experimental data of the C-6 carbons of amylose and inulin and the best fit obtained by using the restricted diffusion model. Clearly, the agreement between the experimental and calculated

values is very good. Table 1 summarizes the optimized parameters of the diffusion model. The correlation times, τ_i , corrected for solvent viscosity are not very different for amylose and inulin. The Arrhenius plots of the correlation times, τ_i , gave comparable apparent activation energies of 14 and 16 kJ mol⁻¹ for inulin and amylose, respectively. Internal rotations are restricted in nature characterized by amplitudes between 120 and 270° for inulin and between 80 and 120° for amylose in the temperature range of 60 and 95 °C for inulin and amylose, respectively. The smaller range of the amplitude 2χ observed in amylose relative to that in inulin indicates that the internal rotation of the hydroxymethyl group in the former polysaccharide is more restricted than in the latter macromolecule. Moreover, the range of the amplitude of internal rotation in amylose is in agreement with the angular range of 120° separating the gauche-gauche and gauche-trans conformations of the hydroxymethyl group about the exocyclic bond observed in the crystal structures of carbohydrates of the gluco configuration.^{10,11} One reviewer raised the interesting question that there might be two asymptotic values for the amplitude, χ , of the restricted internal rotation in amylose at the low (~40 °C) and high temperature (~60 °C) regions (Table 1). However, this is not the case; apart from the propagated experimental error in the calculated χ values, which is estimated to be $\pm 20\%$, the discrepancy of about 20° in the χ values is overlapped by the experimental distribution of the angles O-5-C-5-C-6-O-6 ($+60 \pm 30^\circ$, or $-60 \pm 30^\circ$) observed in the crystal structures of glucopyranosides.^{10,11}

Conclusion. In summary, the present study attempted to describe the backbone rearrangement and the motion of the exocyclic hydroxymethyl group of the linear polysaccharides amylose and inulin in solutions. The DLM model and the restricted diffusion model appear to be a reasonable basis for the present analysis of the relaxation data. Nevertheless, the TCF of the DLM model does not contain parameters derived directly from the specific structural details of the two polysaccharides. What is needed primarily is the formulation of a TCF that can be accounted for explicitly by the geometric constraints of a carbohydrate chain in terms of torsional angles φ and ψ (and ω for 1,6-linkages). The derivation of such a TCF is in progress in our laboratory.

A further, more rigorous quantitative description of the carbohydrate chain dynamics could be performed by employing the orientational TCF for local dynamics developed recently by Perico and co-workers²⁸ on the basis of the optimum Rouse-Zimm approximation (ORZ) to the generalized Langevin diffusion equation in the full configurational space. This theory, the so-called ORZ for local dynamics (ORZLD), involves a structural matrix which contains all the conformational details of

the polymer system. It can be calculated either from the full conformational energy map of the chain or from rotational isomeric state (RIS) models of different degrees of sophistication (RIS-ORZ hierarchy). Thus, the ORZLD model provides the actual form of the TCF, required to interpret the NMR relaxation data, in terms of the specific geometry of a carbohydrate chain. Moreover, this model describes bond motions in the central and end positions of the chain and is able to analyze short-range stiffness for semiflexible polymers.

Acknowledgment. Financial support from the University of Crete is appreciated. E.T. thanks the Research Committee of the University of Crete for fellowship support.

References and Notes

- (1) Dais, P. *Macromolecules* **1985**, *18*, 1351.
- (2) Dais, P. *Carbohydr. Res.* **1987**, *160*, 73.
- (3) Dais, P.; Marchessault, R. H. *Macromolecules* **1991**, *24*, 4611.
- (4) Craik, D. J.; Kumar, A.; Levy, G. C. *J. Chem. Int. Comput. Sci.* **1983**, *1*, 30.
- (5) Schaefer, J. *Macromolecules* **1973**, *6*, 882.
- (6) Valeur, B.; Jarry, J. P.; Geny, F.; Monnerie, L. *J. Polym. Sci., Polym. Phys. Ed.* **1975**, *13*, 667, 2251.
- (7) Jones, A. A.; Stockmayer, W. H. *J. Polym. Sci., Polym. Phys. Ed.* **1977**, *15*, 847.
- (8) Hall, C. K.; Helfand, E. *J. Chem. Phys.* **1982**, *77*, 3275.
- (9) Webber, T. A.; Helfand, E. *J. Chem. Phys.* **1983**, *87*, 2881.
- (10) Dejean, de la Batie, R.; Laupretre, F.; Monnerie, L. *Macromolecules* **1988**, *21*, 2045.
- (11) Winter, W. T.; Sarko, A. *Biopolymers* **1974**, *13*, 1447, 1461.
- (12) Marchessault, R. A.; Perez, S. *Biopolymers* **1979**, *18*, 2369.
- (13) Sundaralingam, M. *Biopolymers* **1968**, *6*, 189.
- (14) Altona, C.; Sundaralingam, M. *J. Am. Chem. Soc.* **1972**, *94*, 8205.
- (15) Marchessault, R. A.; Bleha, T.; Deslandes, Y.; Revol, J.-F. *Can. J. Chem.* **1980**, *58*, 2515.
- (16) Oka, M.; Ota, N.; Nino, Y.; Iwashita, T.; Komura, H. *Chem. Pharm. Bull.* **1990**, *40*, 1203.
- (17) Andre, I.; Pataux, J. L.; Mazeau, K.; Tvaroska, I.; Taravel, F. R.; Chanzy, H., unpublished results.
- (18) French, A. D. *Carbohydr. Res.* **1988**, *176*, 17.
- (19) Kramers, H. A. *Physica* **1940**, *7*, 284.
- (20) Helfand, E. *J. Chem. Phys.* **1971**, *54*, 4651.
- (21) Spyros, A.; Dais, P.; Heatley, F. *Macromolecules* **1994**, *27*, 5845.
- (22) Guillermo, A.; Dupeyre, R.; Cohen-Addad, J. P. *Macromolecules* **1990**, *23*, 1291.
- (23) Gisser, D. J.; Glowinkowski, S.; Ediger, M. D. *Macromolecules* **1991**, *24*, 4270.
- (24) Adolf, D. A.; Ediger, M. D. *Macromolecules* **1991**, *24*, 5834.
- (25) Dais, P.; Nedea, M.-E.; Morin, F. G.; Marchessault, R. H. *Macromolecules* **1989**, *22*, 4208.
- (26) Woessner, D. E. *J. Chem. Phys.* **1962**, *36*, 1.
- (27) Woessner, D. E.; Snowden, B. S.; Meyer, G. H. *J. Phys. Chem.* **1969**, *50*, 719.
- (28) London, R. E. *J. Am. Chem. Soc.* **1978**, *100*, 2678.
- (29) London, R. E. *J. Am. Chem. Soc.* **1978**, *100*, 7159.
- (30) Witterbort, R. J.; Szabo, A. *J. Chem. Phys.* **1978**, *69*, 1722.
- (31) Perico, A. *Acc. Chem. Res.* **1989**, *22*, 336; *Biopolymers* **1989**, *28*, 1527 and references therein.

MA9504680